Robust planning of a European Electricity System under climate uncertainty

Leonie Sara Plaga
Valentin Bertsch
Chair of Energy Systems and Energy Economics
Ruhr-Universität Bochum
44801 Bochum, Germany
Leonie.plaga@ruhr-uni-bochum.de

***Abstract*—Anthropological climate change will lead to significant changes in climate in the coming years. Many components of an energy system depend on climate variables. Yet, projections of future climate are subject to large uncertainties. Hence, in this work a European electricity system is optimized using different climate projections. In addition to single optimizations for the different projections, robust optimizations including all projections are performed. The comparison of the results shows that the different climate projections have significant influence on the electricity system, e.g. the total costs differ by 23.7% between the cheapest and most expensive projection. When planning a robust system including all climate projections, the costs rise by 2.8% compared to the most expensive single projection, avoiding the loss of load for costs of 868 €/MWh. 706 GW of investment decisions are taken regardless of the choice of climate projection and can hence be classified as no-regret investments.**

***Index Terms* – energy system optimization, electricity sector, climate change adaption, robust optimization, uncertainty**

I. INTRODUCTION

Climate scientists project significant changes in climate in the coming years [1]. Global Circulation Models (GCMs), which model physical properties of the atmosphere and the ocean, can project future climate developments, but are subject to large uncertainties due to the complexity of the atmosphere. Energy systems depend on climate variables, as temperature for example influences heating and cooling demand [2]. Therefore, future energy systems should be planned considering climate development and its uncertainties.

There are multiple studies dealing with the influence of climate and its uncertainties [e.g. 2–8]. Yet, among the studies in the field of energy system optimization, the formal assessment of uncertainty in general and climate uncertainty in particular is still rare [9, 10]. Furthermore, the assessment is often limited to either one technology like hydropower [8] or a small geographic area [3].

The European energy system is highly interlinked both among the different technologies as well as geographically, thus, in this study, a European electricity system for the year 2050 is optimized using future climate projections. To assess the uncertainty in the projections, six different climate projections are used in a robust optimization, which ensures that the optimized system meets the demand for all climate projections, while at the same time minimizing the costs of the most expensive projection. Furthermore, we aim to find at which costs robust optimization avoids the loss of load by comparing the costs for robust optimization and the avoided amount of lost load. Finally, investment decisions, which are realized regardless of the climate projection are identified as no-regret investments.

The study is structured as follows: first, the framework for the study and the used climate data and optimization strategy are depicted in Section II. Section III describes the process of converting climate data into energy system input data. In Section IV, results are shown, and Section V contains a conclusion and an outlook on future research.

II. MATERIALS AND METHODS

This section describes the materials and methods, that we used. First, the used energy system model and the data sources for the power system are described. The next section depicts the used climate data followed by a section about the used optimization strategy.

Figure 1: Study area. Dark grey lines mark the borders of the nodes (map created with http://geojson.io)

A. Energy system model and power system data source

To optimize the electricity system, the energy system optimization framework Backbone is used [11]. Backbone is an adaptable framework, that allows for the modelling of different energy systems and already incorporates some

978-1-6654-0896-7/22/$31.00 ©2022 IEEE

tools for scenario based optimization. The power system data and the costs for power system components are exported from the power system optimization model pypsa-eur [12][1]. The study area and the node structure are shown in Figure 1.

Pypsa-eur records the power plant park of 2015. As the European Union plans to be climate neutral by 2050 [13], we assume, that there will be no fossil power plants operating in 2050. Nuclear power plants are decommissioned in Austria, Belgium, Germany and Italy, who decided upon phasing out nuclear. There are investment possibilities in on- and offshore wind, photovoltaic cells as well as battery and hydrogen storage. Nuclear power plants are investment possibilities in all countries which did not phase out nuclear. There are no hydro power and pumped hydro storage investment possibilities due to very limited expansion potential in Europe. There are also no investment possibilities for biomass power plants due to the conflicts with food production. Furthermore, we do not consider grid expansion.

B. Climate Data

Global Circulation Models (GCMs) aim to depict the development of the global climate by modelling oceans and the atmosphere using physical relations. These models provide climate data on large geographic scales. To depict climate development on smaller scales, GCMs can be regionally downscaled by using Regional Climate Models (RCM). The Cordex initiative provides a coordinated framework for regionally downscaled GCMs for the whole globe. In this work, we use climate data from the Euro-Cordex [14], the European branch of the Cordex initiative.

There are many different climate models developed by different institutions. Furthermore, climate models provide projections for different sceanrios of human greenhouse gas emissions. These scenarios follow the Representative Concentration Pathways (RCPs) issued by the IPCC [15]. All climate models of Euro-Cordex report data from 2006 to 2100. The combinations of climate models, RCPs and years used in this study can be found in Table I. The different combinations will be referred to as Projection 1-6 in the following.

Table I: Combinations of climate models, Representative Concentration Pathways (RCPs) and years used in the study. The number in the first column will be used to identify the projection in the following.

Number	*Climate model*	*RCP*	*Year*
1	CNRM-CERFACS-CNRM-CM5	2.5	2046
2	CNRM-CERFACS-CNRM-CM5	2.5	2050
3	CNRM-CERFACS-CNRM-CM5	8.5	2046
4	CNRM-CERFACS-CNRM-CM5	8.5	2050
5	NorESM1-M	2.5	2046
6	NorESM1-M	2.5	2050

C. Optimization Strategy

All combinations of climate models, RCPs and years in Table I depict possible developments of the future climate. Therefore, to design a robust future energy system, all of these projections must be considered. Thus, in this study we use robust optimization. Robust optimization is a tool for optimization under uncertainty where the costs are minimized for the worst possible realization of the uncertain parameters. The objective function obj equals the following:

$$obj = \min\left(c_{\text{invest}} + \max_{p}\ c_{\text{operating}}(p)\right), \qquad (1)$$

where p are the different projections, c_{invest} are the investment costs and $c_{\text{operating}}(p)$ are the projection-specific operating costs [7].

The results of the robust optimization for all six projections are then compared to the results of the single projection optimizations. Furthermore, a robust optimization for only four projections, which are chosen based on the results of the single projection optimization, is conducted. Here, we want to determine how much more expensive the inclusion of additional projections in a robust optimization is.

III. Conversion of Climate Data to Energy System Model Input Data

Many components of an energy system are weather-dependent and therefore also affected by changing climate conditions.

A. Demand

Energy demand is influenced by the temperature as it affects heating and cooling demand. Classifying the dependence of the demand is difficult as it is influenced by many small-scale variables like housing types and consumer's decisions. To overcome these difficulties, regression techniques are common [16–18]. In this study, a quadratic regression was performed on daily historical temperature and demand data to find countrywide dependencies and yielded fair correlation. Examples can be found in the Appendix in Figure 8 and Figure 9.

B. Hydro power

Hydro power generation also depends on weather conditions. The climate models used report the river runoff, which equals the amount of water that drains from land. It is rather difficult to assess hydro power production without looking into site-specific river runoffs, as the hydro power production of a plant depends mainly on the weather conditions of the specific river or basin. Yet, a detailed assessment of all hydro power plants in Europe would go beyond the scope of this study. Therefore, the hydro power production is approximated by using linear regression, similar to [6, 19, 20]. However, performing regression of river runoff and hydro power production on a single country level does not yield significant trends for all European countries. Yet, a trend could be identified on European level (see Appendix Figure 10). From this trend, single country hydro production can be estimated. The procedure for that is shown in the next paragraphs.

[1] The code for the conversion is available at: https://gitlab.ruhr-uni-bochum.de/ee/backbone-tools

First, historical average river runoff $\bar{r}_{\text{hist}}$ in Europe is plotted against the average hourly hydro production gen_{hist} of this month for the years 2010-2015 (see Appendix Figure 10). Then, a linear regression is performed between these two variables using the slope m and the intercept b. With these values, the future hourly hydro power generation gen_{Europe} in Europe can be calculated from the river runoff r_{Europe} with the following equation:

$$gen_{\text{Europe}} = a \cdot r_{\text{Europe}} + b. \tag{2}$$

This equation allows for the calculation of the total hydro production in Europe. To obtain country-specific values, it is assumed, that the ratio of the yearly hydro generation per country and the yearly runoff is constant. For the historic period (2010-2015) this quotient q_c can be obtainted by using the total hydro generation of a country in the historic period $gen_c(\text{hist})$ and the total runoff in this country in the historic period $r_c(\text{hist})$:

$$q_c = \frac{gen_c(\text{hist})}{r_c(\text{hist})}. \tag{3}$$

For the future climate data, this quotient is then modified to account for an in- or decrease in the total European hydro production. Therefore, the total hydro production in Europe $gen_{\text{Eur}}(\text{fut})$ and the total historic hydro production in Europe $gen_{\text{Eur}}(\text{hist})$ as well as the total runoff in Europe for the future year $r_{\text{Eur}}(\text{fut})$ and the total historic runoff in Europe $r_{\text{Eur}}(\text{hist})$ are used to obtain a weighting factor per country f_c:

$$f_c = \frac{gen_c(\text{hist}) \cdot gen_{\text{Eur}}(\text{fut})}{gen_{\text{Eur}}(\text{hist})} \cdot \frac{r_{\text{Eur}}(\text{hist})}{r_c(\text{hist}) \cdot r_{\text{Eur}}(\text{fut})}. \tag{4}$$

With this weighting factor f_c, the hourly hydro production of a country $gen_c(fut)[\text{h}]$ can be determined by using the reported hourly runoff $r_c(\text{fut})[\text{h}]$ with the following equation:

$$gen_c(fut)[\text{h}] = f_c' \cdot r_c(\text{fut})[\text{h}]. \tag{5}$$

C. Wind

Wind speeds vary depending on the height. The climate model reports the wind speed $v(h_0)$ at a height h_0. To calculate the wind speed $v(h)$ at hub height h, the following equation is used:

$$v(h) = v(h_0) \cdot \left(\frac{h}{h_0}\right)^{1/7} \tag{6}$$

The capacity factor c_{f} of the wind turbine is then calculated using standardized production values:

$$c_{\text{f}} = \begin{cases} 0, & v < v_{\text{in}} \\ \dfrac{v^3 - v_{\text{in}}^3}{v_{\text{r}}^3 - v_{\text{in}}^3}, & v_{\text{in}} \le v < v_{\text{r}} \\ 1, & v_{\text{r}} \le v < v_{\text{out}} \\ 0, & v > v_{\text{out}}, \end{cases} \tag{7}$$

where v is the actual velocity, v_{in} is the cut-in velocity, v_{r} is the rated velocity and v_{out} is the cut-out velocity [17].

D. Photovoltaics

The output of photovoltaic (PV) cells depends on the solar irradiation and on the cell temperature, as it influences the cells' efficiency. The power output P of a photovoltaic cell can be calculated by:

$$P = P_{\text{STC}} \cdot \frac{\eta}{\eta_{\text{STC}}} \cdot \frac{G}{G_{\text{STC}}}, \tag{8}$$

with the efficiency η and solar irradiation G. If a variable is indexed with STC, it refers to the value at Standard Testing conditions. The efficiency of the cell depends on the temperature of the cell T_{cell}:

$$\eta = \eta_{\text{STC}}\big(1 - \beta(T_{\text{cell}} - T_{\text{STC}})\big), \tag{9}$$

where β is a coefficient describing the loss of efficiency per temperature rise [3, 17]. The cell temperature can be calculated from the ambient temperature T_{am} and a cell heating coefficient c with the following equation [6]:

$$T_{\text{cell}} = T_{\text{am}} + c \cdot G. \tag{10}$$

E. Thermal power plants

The efficiency of thermal power plants decreases with rising temperatures as thermal power plants rely on cooling water. How much a thermal power plant is affected by changing temperatures depends on the used cooling system: once-through (OT) cooling systems use fresh water from rivers, while closed-loop (CL) cooling systems reuse cooling water. Because they draw their water directly from a reservoir, OT cooling is much more vulnerable to changing temperatures, but also cheaper than CL cooling. In 2014, 43% of US thermal power plants where equipped with OT cooling, while 53% used CL cooling technologies [21]. As OT cooling requires more freshwater resources, we assume, that all European power plants will be equipped with CL cooling systems in 2050. The temperature dependence of their efficiency η can then be calculated using:

$$\eta = \begin{cases} \eta_0, & T \le T_{\text{health}} \\ \eta_0\big(1 - \rho(T - T_{\text{health}})\big), & T > T_{\text{health}}, \end{cases} \tag{11}$$

where T is the actual temperature, T_{health} is the maximum temperature, which allows to the power plant to operate with its rated efficiency η_0 and ρ is the efficiency degrading coefficient [3].

F. Bias adaption

Due to the challenges that occur when such a complex system as the atmosphere is modelled, climate models often show a bias when compared to observed data. In most studies [e.g. 4, 22], bias correction techniques in combination with historical data are used to correct for this bias. In this study, empirical quantile delta mapping is used to correct the bias in wind capacity factors, PV capacity factors and efficiency of thermal power plants. Therefore, for a historic period (2011-2015), wind and PV capacity factors, as well as the efficiencies of thermal power plants are calculated both with the climate model data and ERA5 reanalysis data [23]. Then the quantile delta mapping algorithm as described in [24] is applied to correct for the bias. Demand and hydro production are not bias adapted as they are created using regression techniques with historical data.

IV. RESULTS

In this section, first the differences between the single optimizations of the different climate projections are displayed, followed by the investment decisions and costs for the robust optimization. In the next section, the value of lost load is calculated. The chapter closes with the identification of no-regret investments. Most of the data for the analysis was directly taken from pypsa-eur. All other data can be found in the Appendix in Table II.

A. Influence of climate projections on energy system optimization results

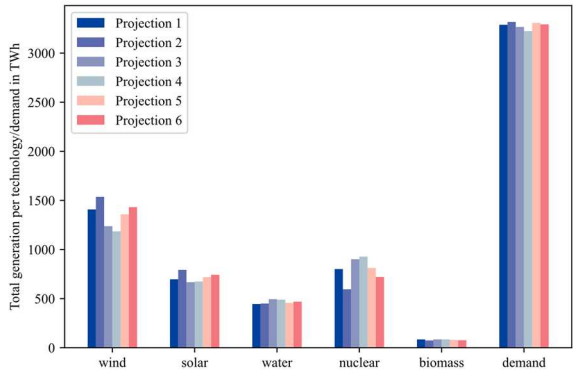

Figure 2: Total electricity generation from different technologies depending on the climate projection.

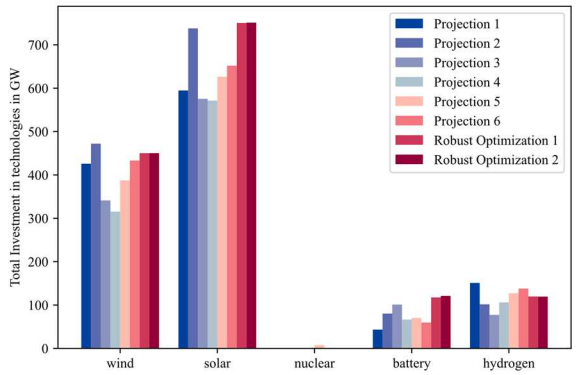

Figure 3: Total investment in different technologies for the six single projection optimizations (Projection 1-6) and the two robust optimizations (Robust optimization 1-2).

Figure 2 shows the electricity generation from different technologies and the demand. The total production from water, biomass and the demand only vary slightly for the different climate projections, but there is notably less wind electricity production for Projection 3 and 4 than for the other projections. Projection 2 shows the lowest production from nuclear power plants, which is compensated by higher wind and solar production. It also has the highest investments in solar and wind power plants as depicted in Figure 3. When looking at the average capacity factors in Figure 4, it shows that the weather conditions for Projection 2 are unfavorable: the average capacity factor for wind energy is 5.4% below the average capacity factor for all projections, the average solar capacity factor is 6.5% below average and the water capacity factor is 3.6% below average. Yet, there is a higher wind and solar production as in other projections, while nuclear power is curtailed. This can be explained as due to the lower capacity factors in Projection 2, more investments in generation capacities are necessary to meet the demand. It appears that despite the lower capacity factors, renewables are still economically preferable to new investments in nuclear powerplants. Even with lower average capacity factors as in Projection 2, there are still timesteps with high capacity factors. At these timesteps, renewable production is preferred over nuclear power, as the variable costs are lower. This causes the unintuitive results that more renewable power is generated in Projection 2 despite the unfavorable capacity factors.

The total annual costs differ among the climate projections: the cheapest projection (Projection 4) results in annual total costs of 156 billion €, while the most expensive projection (Projection 2) results in costs of 193 billion €. The costs for all projections are displayed in Figure 5. The different results of the projections support the need for an optimization strategy that includes all projections.

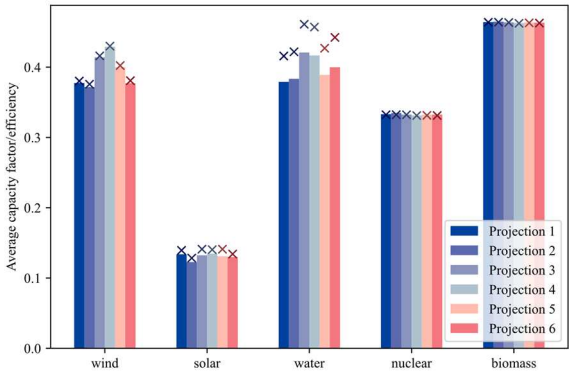

Figure 4: Average capacity factors (wind, solar, water) and efficiencies (nuclear, biomass) for different technologies in the different single projections. The bars show the average capacity factors/efficiencies reached in the simulations while the crosses mark the maximum possible average capacity factors/efficiencies for the projection.

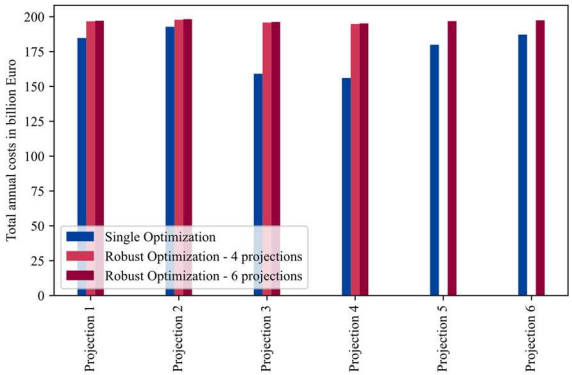

Figure 5: Total annual costs for the six single projection optimizations (Projection 1-6) and the two robust optimizations (Robust optimization 1-2).

B. Robust optimization

After the single projection optimization, two robust optimizations with the objective function reported in Equation (1) are performed, once including Projections 1-4 (Robust optimization 1), and once including Projections 1-6

(Robust optimization 2). The projections for Robust optimization 1 were chosen such that both the cheapest and the most expensive projection were included. Compared to the single optimizations, there is more investment in solar power and batteries (see Figure 3). It appears, that the combination of solar power and batteries is more robust to differing climate than wind power. This is underlined by the smaller variation in capacity factors among the projections for solar power than for wind (see Figure 4).

The robust planning of the energy system comes with additional costs. Compared to the most expensive projection (Projection 2), the increase in costs for Robust optimization 2 is with 2.8% moderate but compared to the cheapest projection (Projection 4), the costs rise by 25.1%. The average cost difference between Robust optimization 1 and 2 accounts for 0.21 % and is hence very low. This is not too surprising as Robust optimization 1 already includes the most extreme projections (2 and 4). Hence, if the energy system is robust to these projections, additional robustness to less extreme projections comes with very low additional costs.

C. *Costs of avoding loss of load*

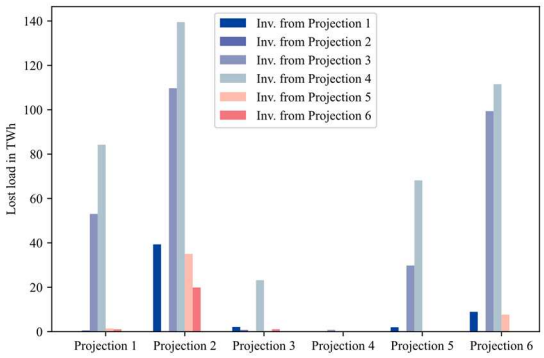

Figure 6: Lost load, if a projection is scheduled with the investment decisions taken for another projection. The x-axis shows the projections that were scheduled, while the color code shows, which investment decisions were chosen.

To put additional costs in relation to the benefits of robust optimization, we take a closer look at the demand, that cannot be met (lost load), when a climate projection is scheduled with investment decisions taken for another projection. Therefore, five scheduling optimizations are performed for each of the six projections using the investment decisions taken for the other climate projections. Figure 6 shows the lost load. The lost load reaches values between 0 and 140 TWh. The average lost load is 23.3 TWh. On average, the additional costs of Robust optimization 2 (where no load is lost for any projection) compared to the single optimizations are 20.2 billion €. This results in an average value of lost load of 868.0 €/MWh.

D. *No-regret investments*

In Figure 7, country-specific investments can be seen. 706 GW of the investments in solar and wind power are the same for all six single and the two robust optimizations. Those can be classified as no-regret investment, as they are chosen regardless of the climate projection. The biggest no-regret investment is solar power in Italy with 257 GW. No-regret investments for storages are shown in Figure 11 (Appendix). There were no no-regret investments in nuclear power, as there were only investments in nuclear power for one projection.

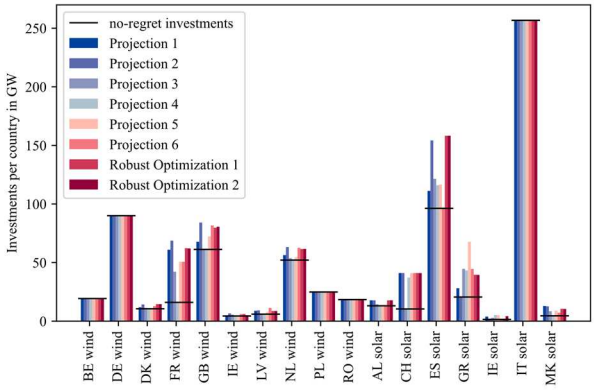

Figure 7: Total investment in wind and solar power per country for the six single projection optimizations (Projection 1-6) and the two robust optimizations (Robust optimization 1-2). The black lines mark no-regret investments. Countries not shown do not have no-regret investments.

V. CONCLUSION AND OUTLOOK

This study examined the influence of uncertainty in climate development on energy systems. Therefore, six different climate development projections were used to optimize the European electricity system. The choice of climate projection influences the outcome of the optimization model, for example the cost difference between the cheapest and most expensive projection account for 37 billion €. Robust optimization, which was used to plan an energy system robust to all climate projections, increases costs on average by 20.2 billion €. Here, more solar power and battery storage is installed compared to single projection optimization, as the capacity factors vary less for solar than for wind among the projections. The average costs for avoiding lost load by robust planning amount to 868.0 €/MWh. In the literature, values of lost load between 1500 €/MWh up to 130000 €/MWh are reported [25, 26]. Here, in any case, robust planning would come cheaper than dealing with the lost load. Finally, 706 GW of no-regret generation investments can be identified.

The study is limited, as it only considers the electricity sector, however the heat sector might be even more influenced by changing temperatures. Electrification in the transport and heating sector will probably also enlarge the electricity demand in the future. Furthermore, some refinements can be made on the conversion routine from climate data to energy system input data. Especially the capacity factors for onshore wind were lower than expected. Here, the choice of different turbine parameters or another method for wind speed interpolation can be useful.

Further research shall be conducted by including more climate projections. To limit computational time, robust optimization shall be combined with techniques to reduce the amount of input data, like Importance Subsampling [27]. Furthermore, a more detailed treatment of the costs of robust optimization and the costs for avoiding lost load is desirable. Finally, as mentioned before, modelling impacts on a sector-coupled system might yield interesting results.

VI. REFERENCES

[1] V. Masson-Delmotte *et al., Climate Change 2021: The Physical Science Basis. Contribution of Working Group I to the Sixth Assessment: Report of the Intergovernmental Panel on Climate Change*: Cambridge University Press, 2021. Accessed: Nov. 3 2021. [Online]. Available: https://www.ipcc.ch/report/sixth-assessment-report-working-group-i/

[2] U. Berardi and P. Jafarpur, "Assessing the impact of climate change on building heating and cooling energy demand in Canada," *Renewable and Sustainable Energy Reviews*, vol. 121, p. 109681, 2020, doi: 10.1016/j.rser.2019.109681.

[3] I. F. Abdin, Y.-P. Fang, and E. Zio, "A modeling and optimization framework for power systems design with operational flexibility and resilience against extreme heat waves and drought events," *Renewable and Sustainable Energy Reviews*, vol. 112, pp. 706–719, 2019, doi: 10.1016/j.rser.2019.06.006.

[4] P. J. Coker, H. C. Bloomfield, D. R. Drew, and D. J. Brayshaw, "Interannual weather variability and the challenges for Great Britain's electricity market design," *Renewable Energy*, vol. 150, pp. 509–522, 2020, doi: 10.1016/j.renene.2019.12.082.

[5] S. Li, D. W. Coit, and F. Felder, "Stochastic optimization for electric power generation expansion planning with discrete climate change projections," *Electric Power Systems Research*, vol. 140, pp. 401–412, 2016, doi: 10.1016/j.epsr.2016.05.037.

[6] S. E. L. Medeiros, P. F. Nilo, L. P. Silva, C. A. C. Santos, M. Carvalho, and R. Abrahão, "Influence of climatic variability on the electricity generation potential by renewable sources in the Brazilian semi-arid region," *Journal of Arid Environments*, vol. 184, p. 104331, 2021, doi: 10.1016/j.jaridenv.2020.104331.

[7] A. Moreira, D. Pozo, A. Street, E. Sauma, and G. Strbac, "Climate-aware generation and transmission expansion planning: A three-stage robust optimization approach," *European Journal of Operational Research*, vol. 295, no. 3, pp. 1099–1118, 2021, doi: 10.1016/j.ejor.2021.03.035.

[8] S. C. Parkinson and N. Djilali, "Robust response to hydro-climatic change in electricity generation planning," *Climatic change*, vol. 130, no. 4, pp. 475–489, 2015, doi: 10.1007/s10584-015-1359-5.

[9] X. Yue, S. Pye, J. DeCarolis, F. G. Li, F. Rogan, and B. Ó. Gallachóir, "A review of approaches to uncertainty assessment in energy system optimization models," *Energy Strategy Reviews*, vol. 21, pp. 204–217, 2018, doi: 10.1016/j.esr.2018.06.003.

[10] J. Cronin, G. Anandarajah, and O. Dessens, "Climate change impacts on the energy system: a review of trends and gaps," *Climatic change*, vol. 151, no. 2, pp. 79–93, 2018, doi: 10.1007/s10584-018-2265-4.

[11] N. Helistö *et al.,* "Backbone—An Adaptable Energy Systems Modelling Framework," *Energies*, vol. 12, no. 17, p. 3388, 2019, doi: 10.3390/en12173388.

[12] J. Hörsch, F. Hofmann, D. Schlachtberger, and T. Brown, "PyPSA-Eur: An open optimisation model of the European transmission system," *Energy Strategy Reviews*, vol. 22, pp. 207–215, 2018, doi: 10.1016/j.esr.2018.08.012.

[13] European Union, "REGULATION (EU) 2021/1119 OF THE EUROPEAN PARLIAMENT AND OF THE COUNCIL: establishing the framework for achieving climate neutrality and amending Regulations (EC) No 401/2009 and (EU) 2018/1999 ('European Climate Law')," 2021. Accessed: Apr. 21 2022. [Online]. Available: https://eur-lex.europa.eu/legal-content/EN/TXT/?uri=CELEX:32021R1119

[14] D. Jacob *et al.,* "EURO-CORDEX: new high-resolution climate change projections for European impact research," *Reg Environ Change*, vol. 14, no. 2, pp. 563–578, 2014, doi: 10.1007/s10113-013-0499-2.

[15] IPCC, "Climate Change 2014: Synthesis Report. Contribution of Working Groups I, II and III to the Fifth Assessment Report of the Intergovernmental Panel on Climate Change," Geneva, Switzerland, 2014. Accessed: May 11 2022. [Online]. Available: https://www.ipcc.ch/report/ar5/syr/

[16] K. Handayani, T. Filatova, Y. Krozer, and P. Anugrah, "Seeking for a climate change mitigation and adaptation nexus: Analysis of a long-term power system expansion," *Applied Energy*, vol. 262, p. 114485, 2020, doi: 10.1016/j.apenergy.2019.114485.

[17] K. van der Wiel, L. P. Stoop, B. van Zuijlen, R. Blackport, M. A. van den Broek, and F. M. Selten, "Meteorological conditions leading to extreme low variable renewable energy production and extreme high energy shortfall," *Renewable and Sustainable Energy Reviews*, vol. 111, pp. 261–275, 2019, doi: 10.1016/j.rser.2019.04.065.

[18] Y. Zhang and B. M. Ayyub, "Electricity System Assessment and Adaptation to Rising Temperatures in a Changing Climate Using Washington Metro Area as a Case Study," *J. Infrastruct. Syst.*, vol. 26, no. 2, p. 4020017, 2020, doi: 10.1061/(ASCE)IS.1943-555X.0000550.

[19] O. J. Guerra, D. A. Tejada, and G. V. Reklaitis, "Climate change impacts and adaptation strategies for a hydro-dominated power system via stochastic optimization," *Applied Energy*, 233-234, pp. 584–598, 2019, doi: 10.1016/j.apenergy.2018.10.045.

[20] G. Zhao, H. Gao, and S.-C. Kao, "The implications of future climate change on the blue water footprint of hydropower in the contiguous US *," *Environ. Res. Lett.*, vol. 16, no. 3, p. 34003, 2021, doi: 10.1088/1748-9326/abd78d.

[21] S.-Y. Pan, S. W. Snyder, A. I. Packman, Y. J. Lin, and P.-C. Chiang, "Cooling water use in thermoelectric power generation and its associated challenges for addressing water-energy nexus," *Water-Energy Nexus*, vol. 1, no. 1, pp. 26–41, 2018, doi: 10.1016/j.wen.2018.04.002.

[22] S. Kozarcanin, H. Liu, and G. B. Andresen, “21st Century Climate Change Impacts on Key Properties of a Large-Scale Renewable-Based Electricity System,” *Joule*, vol. 3, no. 4, pp. 992–1005, 2019, doi: 10.1016/j.joule.2019.02.001.
[23] J. Muñoz Sabater, *ERA5-Land hourly data from 1981 to present.* [Online]. Available: doi.org/10.24381/cds.e2161bac (accessed: Oct. 5 2021).
[24] A. J. Cannon, S. R. Sobie, and T. Q. Murdock, “Bias Correction of GCM Precipitation by Quantile Mapping: How Well Do Methods Preserve Changes in Quantiles and Extremes?,” *J. Climate*, vol. 28, no. 17, pp. 6938–6959, 2015, doi: 10.1175/JCLI-D-14-00754.1.
[25] Swinand, G. Peter, Natraj, and Ashwini, “The Value of Lost Load (VoLL) in European Electricity Markets: Uses, Methodologies, Future Directions,” in *16th International Conference on the European Energy Market (EEM): 18-20 September 2019, Ljubljana, Slovenia*, Ljubljana, Slovenia, 2019, pp. 1–6.
[26] T. Schröder and W. Kuckshinrichs, “Value of Lost Load: An Efficient Economic Indicator for Power Supply Security? A Literature Review,” *Front. Energy Res.*, vol. 3, p. 55, 2015, doi: 10.3389/fenrg.2015.00055.
[27] A. P. Hilbers, D. J. Brayshaw, and A. Gandy, “Importance subsampling: improving power system planning under climate-based uncertainty,” *Applied Energy*, vol. 251, p. 113114, 2019, doi: 10.1016/j.apenergy.2019.04.110.
[28] P. Henckes, C. Frank, N. Küchler, J. Peter, and J. Wagner, “Uncertainty estimation of investment planning models under high shares of renewables using reanalysis data,” *Energy*, vol. 208, p. 118207, 2020, doi: 10.1016/j.energy.2020.118207.

VII. APPENDIX

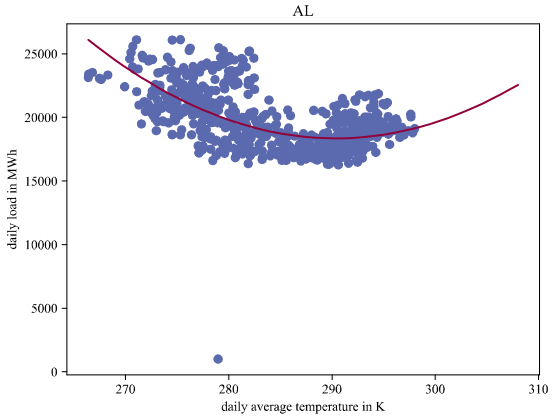

Figure 8: Relation between daily load and average daily temperature for the climate model CNRM-CERFACS-CNRM-CM5 and RCP 8.5 for the country Albania. The red line marks a quadratic regression function.

Table II: Data used for all simulations

Variable	*Value*	*Unit*	*Reference*
h_0 (onshore)	135	m	[28]
v_{in} (onshore)	3	m/s	[28]
v_r (onshore)	14	m/s	[28]
v_{out} (onshore)	25	m/s	[28]
h_0 (offshore)	114	m	[28]
v_{in} (offshore)	4	m/s	[28]
v_r (offshore)	13	m/s	[28]
v_{out} (offshore)	25	m/s	[28]
c	0.03125	Km^2/W	[6]
G_{STC}	1000	W/m^2	[3]
T_{STC}	298	K	[3]
β	0.005	1/K	[3]
ρ	0.0044	1/K	[3]
T_{health}	283	K	[3]

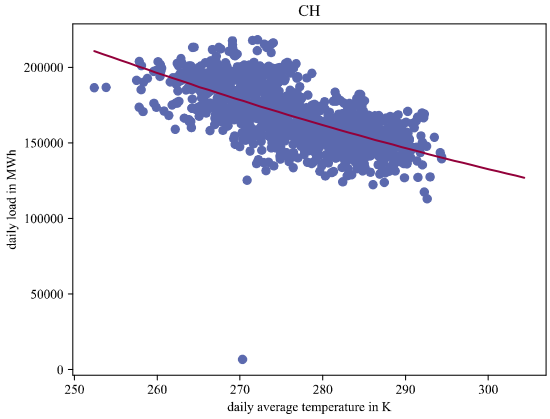

Figure 9: Relation between daily load and average daily temperature for the climate model CNRM-CERFACS-CNRM-CM5 and RCP 8.5 for the country Switzerland. The red line marks a quadratic regression function.

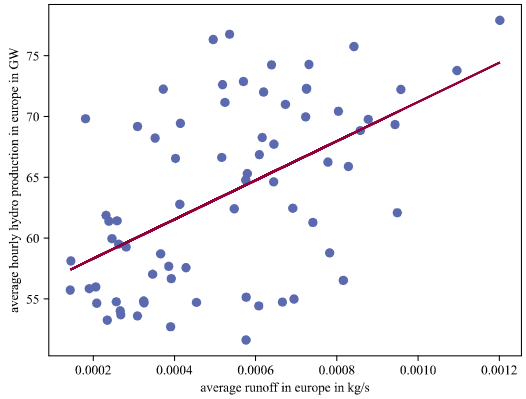

Figure 10: Average river runoff in Europe plotted against average hourly hydro production for the years 2010-2015 in blue dots for the climate model CNRM-CERFACS-CNRM-CM5 and RCP 8.5. The red line marks a linear regression function.

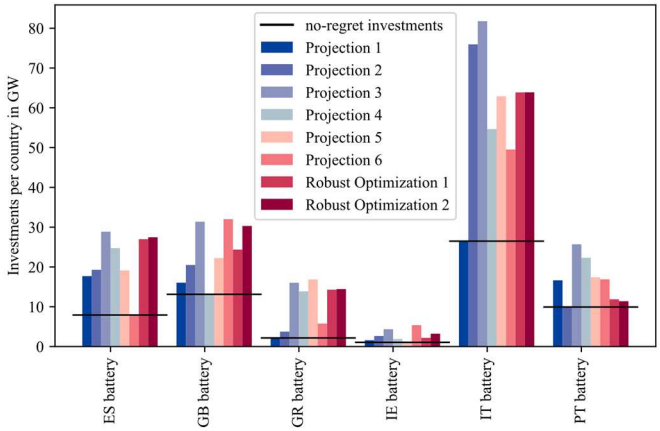

Figure 11: Total investment in battery and hydrogen storage per country for the six single projection optimizations (Projection 1-6) and the two robust optimizations (Robust optimization 1-2). The black lines mark no-regret investments. Countries not shown do not have no-regret investments.